Hindawi
Advances in Materials Science and Engineering
Volume 2018, Article ID 3563914, 12 pages
https://doi.org/10.1155/2018/3563914

Research Article

In Situ Testing of Square Footing Resting on Geobelt-Reinforced Gravel Thin Cushion on Soft Silt

Wei Zhang[1], **David Du**[1,2] **and Xiaohong Bai**[1]

[1]*Department of Civil Engineering, Taiyuan University of Technology, Taiyuan, Shanxi 030024, China*
[2]*Subsea 7 (US) LLC, 17220 Katy Freeway, Suite 100, Houston, TX 77094, USA*

Correspondence should be addressed to Xiaohong Bai; bxhong@tyut.edu.cn

Received 18 October 2017; Revised 16 April 2018; Accepted 18 April 2018; Published 10 May 2018

Academic Editor: Michael Aizenshtein

A series of in situ static loading tests of square footing were carried out on the geobelt-reinforced gravel cushion on soft silt. The reinforced gravel cushion was thin with the depth-to-width ratio of 0.2. A parameters study was conducted by considering the number of geobelt layers, the depth of the first geobelt layer beneath the footing, the vertical spacing between two geobelt layers, the linear density of reinforcement, and the material type of geobelt. The pressure distribution on bottom of the cushion was measured. The test results showed that the bearing capacity of reinforced gravel cushion was significantly larger than that of unreinforced gravel cushion, and the stress diffusion effect of reinforced gravel cushion was also more pronounced than that of the unreinforced cushion. The pressure distribution on bottom of reinforced gravel cushion was in a saddle shape. According to calculation and analysis, the stress diffusion angles of reinforced cushions were all larger than 20°.

1. Introduction

For using it as foundation, soft silt soil has to be treated due to its low bearing capacity and large settlement. An effective treatment is to replace a shallow depth of upper soft silt with geosynthetic-reinforced gravel cushion, which is cost-effective compared to other conventional methods [1, 2]. It has been demonstrated that geosynthetic reinforcement can improve the bearing capacity and reduce uneven settlement of the foundation [3–5]. By conducting 65 groups of model tests, Binquet and Lee [6, 7] first reported that, by reinforcing sand layer underneath the strip footing with strips of aluminum foil, the settlement and ultimate bearing capacity of the foundation was greatly improved. In literatures[8–14], similar results were reported by researchers. It should be noted that it is complicated to determine the ultimate bearing capacity of square footing on reinforced soil. In addition, there has been limited research investigating the stress diffusion effect of reinforced cushion.

For determining the bearing capacity and stress diffusion capacity, most studies have used small-scale models test, which would have size effect and limitations to reflect the actual behaviors of the deformation and bearing capacity of foundation [15–17]. Therefore, it is imperative to conduct full-scale in situ tests to investigate the effects of reinforcing geosynthetic materials. In the literature, geotextiles including geogrid [17–19], geonet [20], geocell [21, 22], and fiber [23, 24] are commonly used as reinforcing materials, while geobelt, a relatively new material, has been rarely utilized. Moreover, most of the previous studies have focused on the settlement and bearing capacity of foundation [1, 6, 9, 12, 15, 25], while little attention has been paid to the stress diffusion angle of reinforced cushion. In practical, due to presence of geobelt, the overall rigidity and stress diffusion capacity of the reinforced cushion can be greatly improved even for thin cushions. Therefore, based on the stress diffusion theory of double-layered foundation, this study aims to investigate the bearing capacity and earth pressure distribution of square footing resting on the thin gravel cushion through a series of in situ static loading tests. The stress diffusion effect of geobelt on the reinforced gravel cushion was also studied.

Table 1: Physical and mechanical parameters of silt soil.

γ(kN/m^3)	γ_D(kN/m^3)	G_S	e	ω(%)	ω_L(%)	ω_p(%)	E_S(MPa)	f(MPa)
18.9	14.5	2.69	0.881	31.8	32.9	23.7	3.93	70

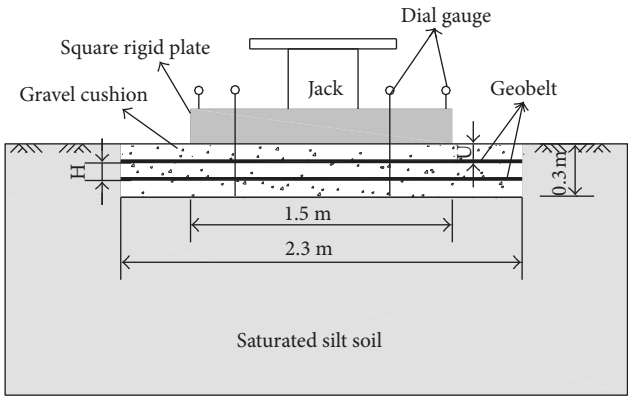

Figure 1: Setup of the loading test.

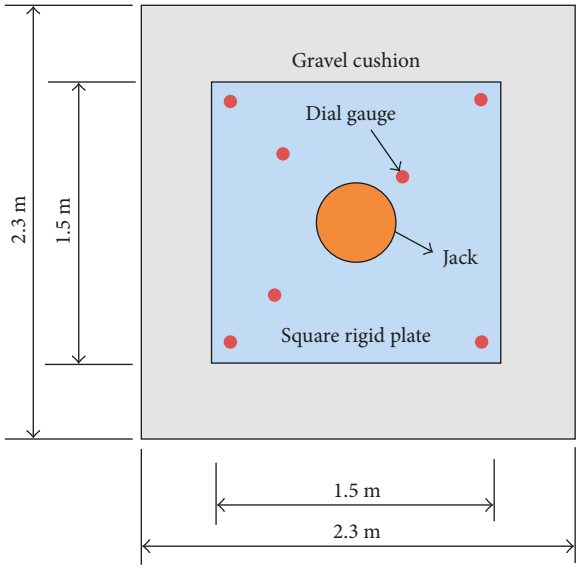

Figure 2: Top view of the testing setup.

2. Experiment

2.1. Test Design and Setup. The testing site, with a dimension of 30 m × 17 m, is located in southwest part of Taiyuan city, China. In the testing site, the natural soil beneath the gravel cushion was saturated soft silt soil. The properties of the silt soil are listed in Table 1.

Each static loading test was conducted on the field test pit with a length of 2.3 m and width of 2.3 m within the testing site. Figure 1 shows the layout of the test setup. A steel square rigid plate with a length of 1.5 m, width of 1.5 m, and depth of 0.3 m was used as a footing to apply the loading. A gravel cushion with a dimension of 2.3 m × 2.3 m × 0.3 m with or without geobelt reinforcement was prepared before each loading test. The loading was applied by a mechanical jack-beam loading system on the gravel cushion through the square footing.

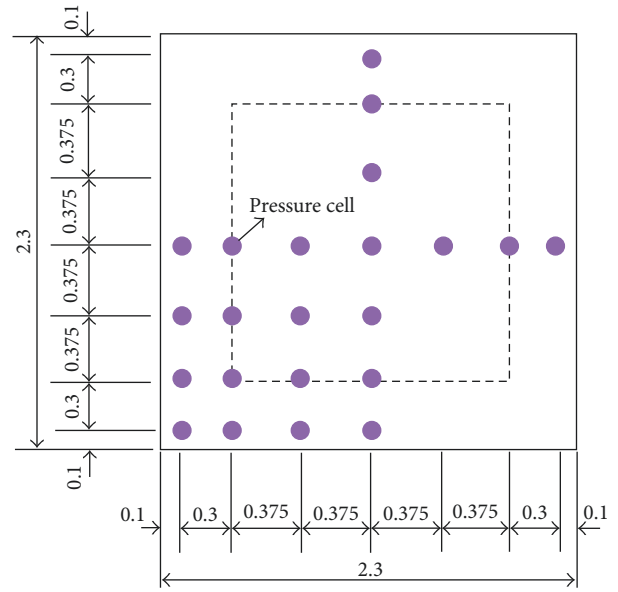

Figure 3: Distribution of pressure cells (unit: m).

Table 2: Testing program.

Test number	N^*—	U^* (mm)	H^* (mm)	LDR* (%)	Material type
A0	Unreinforced	—	—	—-	—
A1-1	1	50	—	33.3	TG
A1-2	1	100	—	50.0	TG
A1-3	1	100	—	33.3	TG
A1-4	1	100	—	25.0	TG
A1-5	1	200	—	33.3	TG
A2-1	2	50	100	33.3	TG
A2-2	2	50	150	33.3	TG
B2-1	2	50	100	33.3	CPE
B2-2	2	50	150	33.3	CPE

$^*N$ represents the layers of geobelt set in the gravel cushion, U is the depth of the first geobelt layer beneath the footing, H refers to the vertical spacing between two layers of geobelt, and LDR is the linear density of reinforcement which means the ratio of the width of geobelt to the center spacing of two geobelts.

Seven dial gauges were deployed in each test, as shown in Figure 2. Four gauges were attached on the four corners of the square rigid plate to measure the overall settlement of the footing. Other three gauges were attached on the bottom of the gravel cushion to monitor the settlement of silt soil. The deformation of the gravel cushion can then be calculated according to the measurements of seven gauges. As shown in Figure 3, twenty-two pressure cells, with a measuring capacity of 0.6 MPa, were deployed on the bottom of the gravel cushion to measure the pressure of the cushion resting on silt soil during loading.

In total, 10 in situ tests were conducted on unreinforced and geobelt-reinforced gravel cushions over saturated silt soil. The testing programs are summarized in Table 2.

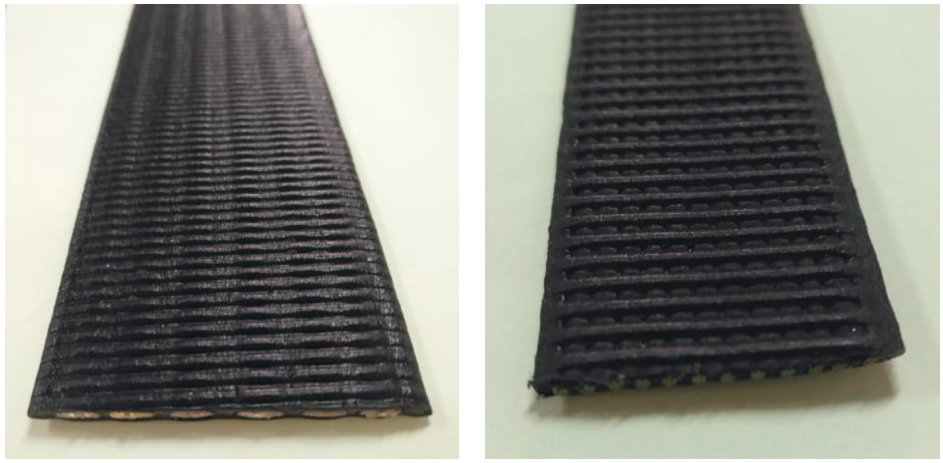

(a) (b)

Figure 4: Photo of geobelts: (a) TG geobelt; (b) CPE geobelt.

Table 3: Engineering properties of the geobelts.

	TG geobelt	CPE geobelt
Geometry size (mm × mm)	25 × 2.5	25 × 2.0
Ultimate tensile strength (MPa)	95.4	139.4
Modulus at strain = 2% (MPa)	10,373	15,064
Length per kilogram (m/kg)	>16	>12
Fracture strain (%)	0.85	1.89
Breaking load (kN)	5.96	6.97
Wrapping material	Polyolefin	Chlorinate polyethylene
Inner material	Glass fiber	Galvanized steel wire

2.2. Materials

2.2.1. Geobelts. Two types of geosynthetic materials used in this study are TG geobelt and CPE geobelt. TG geobelt, as shown in Figure 4(a), is mainly made of fiberglass coated with polyolefin. As shown in Figure 4(b), CPE geobelt is high-strength galvanized iron wires coated with chlorinated polyethylene. These two geobelts have high tensile strength, low expansion, and small creep and are resistant to bending fatigue, tension stress crack, bearing, and punching. Moreover, the geobelt has properties such as antiaging, acid/alkali resistance, and suitability for burying in soil. From construction perspective, the geobelts have the advantages of light-weight, simple construction, and shorter construction period. There are rough details and ribs on the surface of two types of geobelt materials for improving the bonding between geobelts and gravel. Their engineering properties are listed in Table 3.

In the test, in order to ensure strong bonding between geobelts and the gravel, the geobelts are bent at both ends by using a sand bag which is around 550~600mm and then fixed by two clamps, as shown in Figure 5. Therefore, the effective length of the geobelt used in the cushion is around 3.5m, including the width of the cushion and the fixing length at both ends.

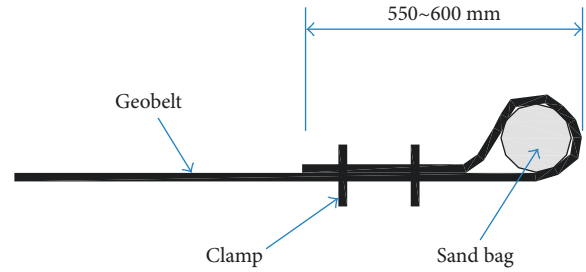

Figure 5: Fixing of geobelt ends.

2.2.2. Gravel Cushion. The thin cushion consisted of gravels with diameter in the range of 10mm– 30mm. Particle size distribution of the gravels is shown in Figure 6. The physical parameters obtained in laboratory tests are listed in Table 4, in which the maximum dry density and optimum moisture content were determined by Standard Proctor Test. According to USCS and AASHTO classification, the gravel was classified as poorly graded gravel (GP).

2.3. Test Procedure. To ensure that each test was conducted under same conditions, the following preparations have to be done. First, the testing pits were dug, cleaned, and leveled to make sure their sizes meet the requirements. Secondly, the sorted fine sand was paved, compacted, and leveled on the bottom of the pits with a thickness of 10 mm~15 mm for reducing stress concentration in the pressure cell. Then the pressure cells were put on the preset positions. The pressure cells should be waterproof and calibrated before each test. Six layers of gravel were paved on the pressure cell with each layer about 50 mm thick. Each layer of gravel in the loose state had the same weight and was then compacted to same compactness by using a wood hammer. Geobelts were laid on the specified position in the gravel cushion with the required linear density of reinforcement (LDR) in two dimensions. The geobelts should be tightened and straightened. A layer of fine sand with a thickness of 10 mm~20 mm was paved above and beneath the geobelts for protecting

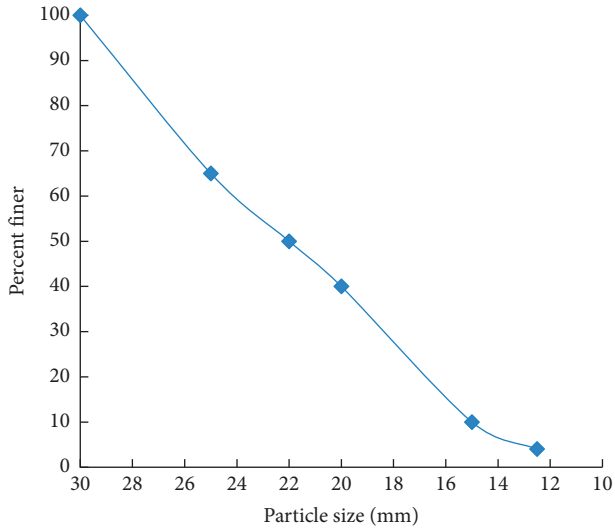

Figure 6: Particle size distribution of the gravel.

Table 4: Physical parameters of gravel.

ρ_{dmax}(kg/m^3)	c_c	c_u	D_{10}(mm)	D_{50}(mm)	ω_{op}(%)
1800	1.92	1.02	15	22	6.8

them from not being punctured by gravel. Geobelts and gravel were laid alternately according to the requirements until the cushion height reached 300 mm. Then the loading plate was put on the top of the reinforced gravel cushion, leveled, and centered properly, to ensure that the load can be evenly distributed on the gravel cushion.

The static loading was applied by using a hydraulic jack. The loading method and stability criteria followed the *Code for Design of Building Foundation* (GB 50007-2011) [26]. The loading was applied with an increment of 20 kPa. If it was less than 0.1 mm/h in two hours, the settlement was recognized to meet the criteria and the next increment of loading can be applied. The test was terminated when the total settlement reached 0.06 B, that is, 90 mm in this program.

After one test was completed, a new test pit was dug in adjacent locations within the testing site. Identical testing procedures were used to perform each test.

3. Test Results and Analysis

3.1. Reinforcing Effect on Bearing Capacity of Foundation. Figure 7 shows pressure-settlement curves of foundations with and without geobelts. It can be seen that the settlement increased with the increase of pressure for both reinforced and unreinforced cushions. However, cushion reinforced with two geobelt layers showed the slowest increase rate of settlement, while unreinforced cushion showed the quickest increase rate. The results indicate that the bearing capacity can be effectively improved by geobelt reinforcement. The reason is that the lateral restraint of geobelt on gravel cushion can decrease the settlement of the gravel cushion, and thus improve the bearing capacity of the foundation compared to the unreinforced cushion. At early stage, the

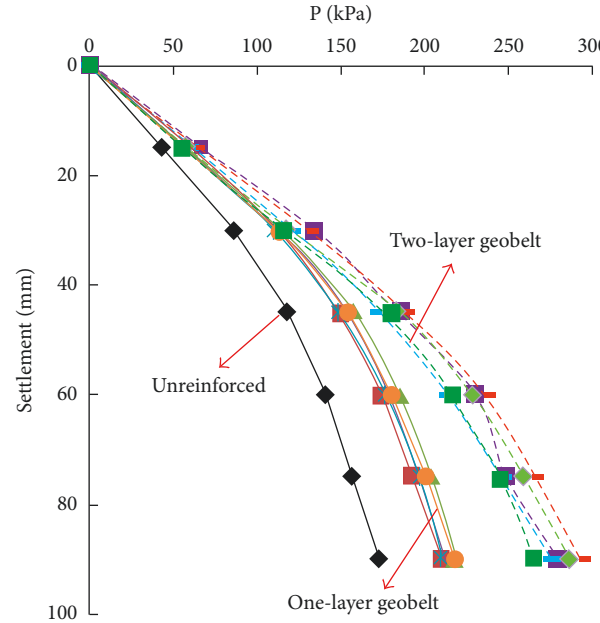

Figure 7: Pressure-settlement curves of cushions with and without geobelts.

settlement increased linearly with pressure. As pressure increased, geobelt comes into play and decreases settlement effectively.

Since no abrupt increase of settlement was observed in all tests, the ultimate bearing capacity of foundation was determined when the settlement of foundation reached 0.06 B (B is the length of the square footing).

To account for the size effect of footing, the bearing capacity ratio (BCR) recommended by Binquet and Lee was calculated as following:

$$\mathrm{BCR} = \frac{q_R}{q_0}, \tag{1}$$

in which q_R and q_0 are the bearing capacity for reinforced and unreinforced soil, respectively. For convenience, the test results were analyzed according to the BCRs calculated at different settlement ratios (s/B). The settlement ratio is calculated by dividing settlement of footing (s) with the width of footing (B). The values of BCR at settlement ratios (s/B) of 0.01, 0.02, 0.03, 0.04, 0.05, and 0.06 are listed in Table 5. The BCR for one-layer geobelt reinforcement was between 1.22 and 1.37, and gradually decreased with the increase of the settlement ratio; the BCR of two-layer geobelt reinforcement was between 1.34 and 1.70 and gradually increased with the increase of the settlement ratio. In current study, the values of BCR are lower than that proposed by Adams and Collin [27], and Chen et al.[28]. This may be due to the relatively small thickness of the cushion used in this study.

Figures 8(a) and 8(b) show the relationship between the number of reinforced layers (N) and BCR. As can be seen, two-layer geobelt reinforcement was much better than one-layer geobelt reinforcement, especially at the late stage of loading. At s/B of 0.06, BCRs of one-layer reinforcement were from 1.22 to 1.26, while for two-layer reinforcement, they were from 1.62 to 1.70, which indicates that the bearing

Table 5: The summary of test results.

Test number	$s/B = 0.01$		$s/B = 0.02$		$s/B = 0.03$		$s/B = 0.04$		$s/B = 0.05$		$s/B = 0.06$	
	q (kPa)	BCR	q (kPa)	BCR	q (kPa)	BCR	q (kPa)	BCR	q (kPa)	BCR	q (kPa)	BCR
A0	43.4	1.00	86.2	1.00	117.7	1.00	140.6	1.00	156.7	1.00	172.6	1.00
A1-1	59.5	1.37	115.4	1.34	150.5	1.28	174.2	1.24	192.5	1.23	210.3	1.22
A1-2	58.2	1.34	114.3	1.33	157.4	1.34	185.2	1.32	204.2	1.30	218.2	1.26
A1-3	56.6	1.30	112.7	1.31	153.0	1.30	180.0	1.28	198.4	1.27	213.4	1.24
A1-4	56.1	1.29	110.2	1.28	148.5	1.26	177.1	1.26	198.1	1.26	210.6	1.22
A1-5	55.2	1.27	112.7	1.31	154.2	1.31	180.0	1.28	201.1	1.28	218.1	1.26
A2-1	67.3	1.55	134.5	1.56	183.9	1.56	230.9	1.56	249.0	1.59	279.8	1.62
A2-2	63.8	1.47	131.4	1.52	188.5	1.60	236.1	1.68	265.5	1.69	293.6	1.70
B2-1	60.3	1.39	120.8	1.40	173.3	1.47	214.4	1.53	245.8	1.57	276.3	1.60
B2-2	58.1	1.34	118.4	1.37	184.3	1.57	228.5	1.63	258.3	1.65	286.7	1.66

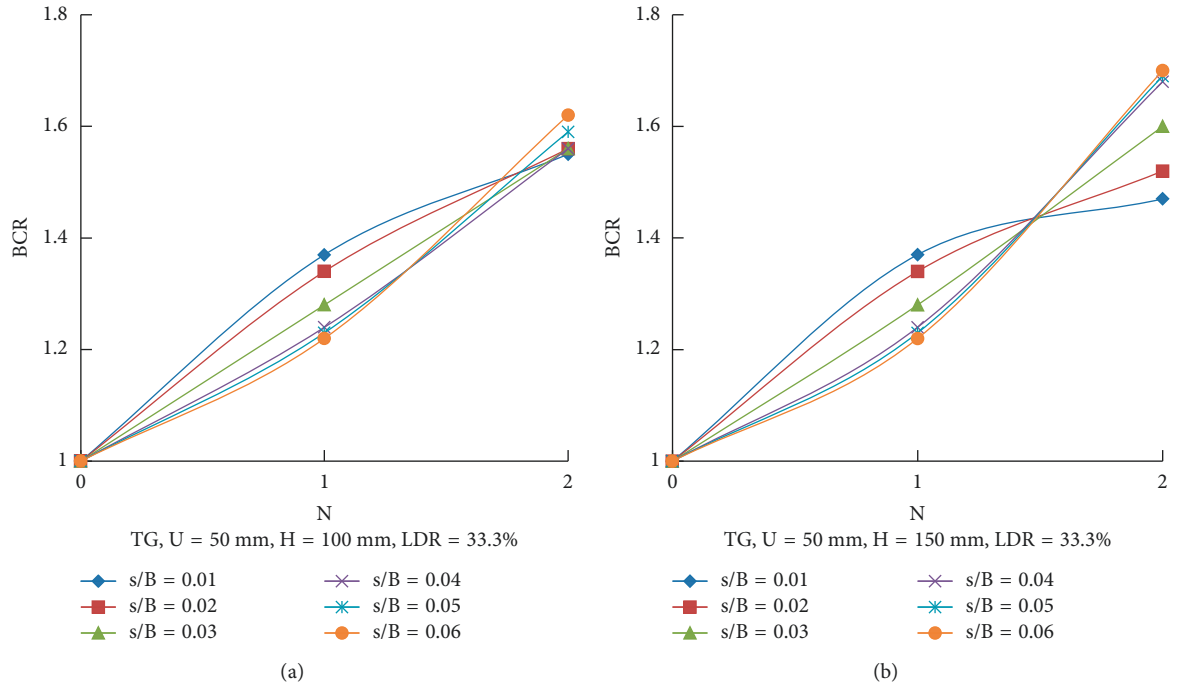

Figure 8: The relationship between BCR and N: (a) TG, $U = 50$ mm, $H = 100$ mm, and LDR = 33.3%; (b) TG, $U = 50$ mm, $H = 150$ mm, and LDR = 33.3%.

capacity of soil reinforced with two-layer geobelt can be increased more at the limit state.

Figure 9 shows the relationship between BCR and the depth of the first geobelt layer beneath the footing (U). At the initial stage of loading ($s/B \leq 0.2$), BCR reached the maximum at 50 mm (U), and gradually decreased as U increased. At the later stage of loading ($s/B \geq 0.3$), BCR slightly increased and the bearing capacity of cushion was improved. This can be explained that the geobelt comes into play after certain amount of settlement happened. In addition, the geobelt could take the effect earlier if it is closer to the footing.

Figure 10 shows the relationship between BCR and the linear density of the reinforcement (LDR). As can be seen, BCR increased slightly with the increase of LDR. When LDR increased from 25% to 50%, the value of BCR increased from (1.22~1.29) to (1.26~1.34). This can be ascribed to the increase of shear strength since the interactions between the geobelt and gravel is improved when LDR is increased which provides more lateral restraint to the gravel cushion.

Figures 11(a) and 11(b) demonstrate the relationship between BCR and vertical spacing (H) for two-layer geobelt-reinforced cushion. At the initial stage of loading ($s/B \leq 0.2$), BCR decreased with the increase of H, while at the later stage ($s/B \geq 0.3$), BCR increased with the increase of H. The results also indicate that the geobelt takes effect when certain amount of settlement happened. At the later stage of loading, reinforcing effect of the geobelt became more pronounced as there was a continuous increase of deformation of the cushion.

Figures 12(a) and 12(b) show the bearing capacity ratio against the settlement ratio for the cushion reinforced with the TG geobelt and CPE geobelt to compare their reinforcing effects. At the initial stage of loading, in terms of bearing

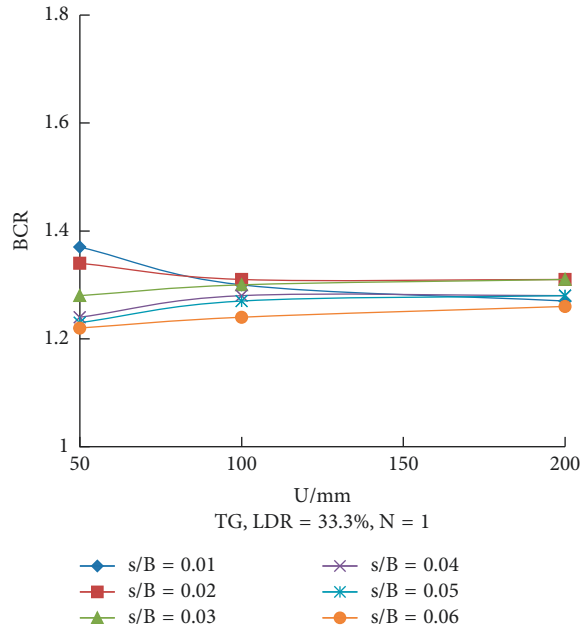

Figure 9: The relationship between BCR and U (TG; LDR = 33.3%; $N = 1$).

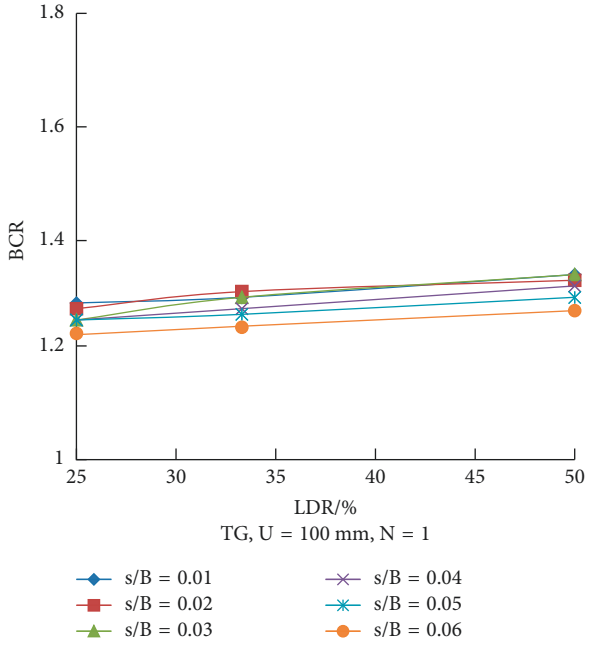

Figure 10: The relationship between BCR and LDR (TG; $U = 100$ mm; $N = 1$).

capacity, the TG-type geobelt performed better than the CPE-type geobelt. However, the difference between them became unnoticeable with the increase of loading.

3.2. Stress Distribution at the Bottom of Reinforced Cushions. Figure 13(a) shows the stress distribution on bottom of the unreinforced gravel cushion. Figures 13(b) and 13(c) show stress distribution on bottom of the reinforced gravel cushion under different pressures. As can be seen in Figure 13(a), for the unreinforced gravel cushion, the stress distribution on bottom of the cushion was parabolic with maximum net earth pressure reached at the center of the cushion. The stress distribution curves on bottom of the reinforced cushion were both in saddle shape and the maximum earth pressures were found to be about 370 mm (one-layer geobelt) and 750 mm (two-layer geobelt) away from the center with the minimum pressure at the center. For the unreinforced cushion, surrounding soft silt soil could not provide strong constrain. As loading increases, the gravels on bottom edges of the footing could be easily pushed out laterally since the pressure on bottom could not be adjusted by the unreinforced cushion itself. While for reinforced cushions, the geobelt restricted the lateral displacement of the cushion owing to frictions between the geobelt and gravels. Therefore, it was not easy to push out the soils located on bottom edges of the footing. The results indicate that, due to using the geobelt, the stress distribution was improved. The central reaction force was decreased, and the edge reaction force was increased. For one-layer and two-layer reinforced cushions (Figures 13(b) and 13(c)), it can be found that, compared to the one-layer cushion, the pressure on the edges of the two-layer reinforced cushion dramatically increased and the pressure distribution became smoother. It is clear that in terms of the reinforcing effect, the two-layer reinforcement is much better than the one-layer reinforcement.

3.3. Stress Diffusion Angle of Cushion. As shown in Figure 13, the earth pressure measured on bottom of the cushions was not evenly distributed. So in this section, the average pressure on the bottom of cushion was calculated according to the measured settlement results which are more accurate and uniform. In same stress path, there exists a one-to-one relationship between settlement and pressure of soil layers. Therefore, the average pressure (P_z) under the cushion can be obtained by using the pressure-settlement curves of natural ground without cushion and with upper cushion, as shown in Figure 14. When the settlement of natural ground under the cushion was equivalent to that of natural ground without the cushion, the corresponding relationship between the pressure P_0 under the cushion and the load P_y on the top of natural ground was obtained; that is, P_y is equal to the mean earth pressure of cushions P_z. Based on the principle of stress diffusion (Figure 15), the stress diffusion angle of the reinforced cushion can be calculated by the following formula:

$$P_0 B^2 = P_Z (B + 2Z \tan\theta)^2,$$

$$\tan\theta = \frac{B}{2Z}\left(\sqrt{\frac{P_0}{P_z} - 1}\right). \quad (2)$$

To investigate the effect of geobelt on stress diffusion, a ratio SDR was defined, in this study, by dividing the stress diffusion angle of the geobelt reinforced cushion with that of the unreinforced cushion. Table 6 lists stress diffusion angles

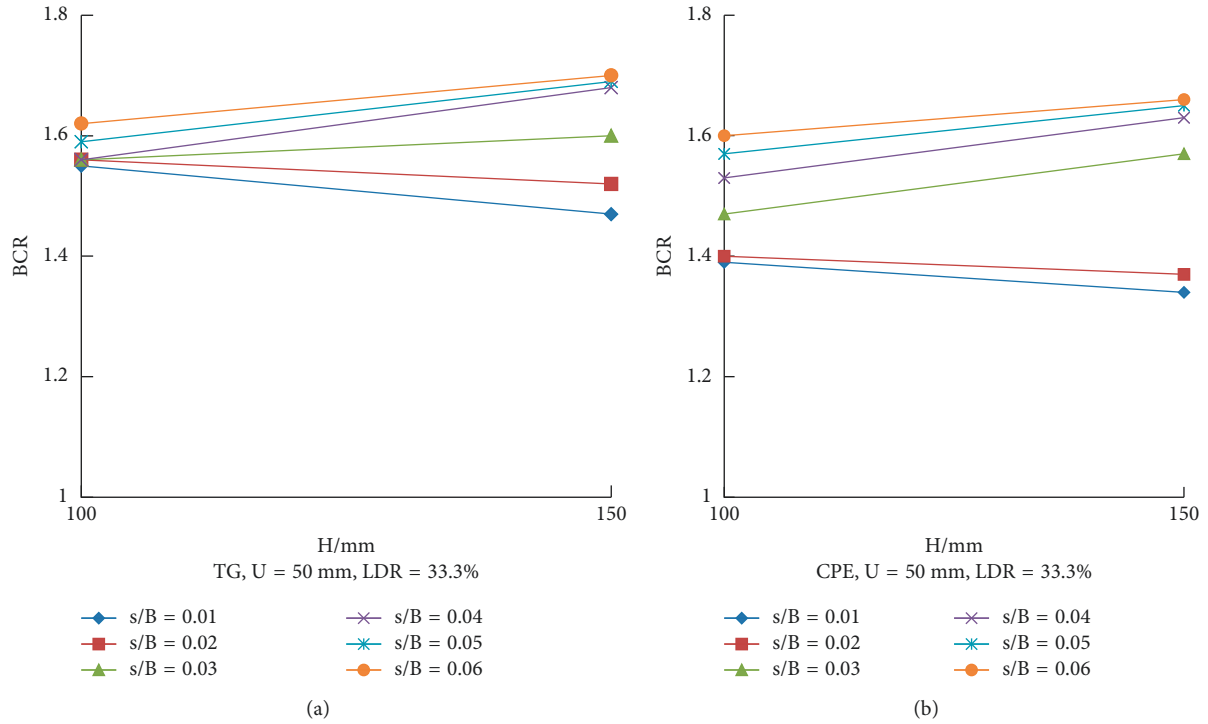

Figure 11: The relationship between BCR and H: (a) TG geobelt ($U = 50$ mm; LDR = 33.3%); (b) CPE geobelt ($U = 50$ mm; LDR = 33.3%).

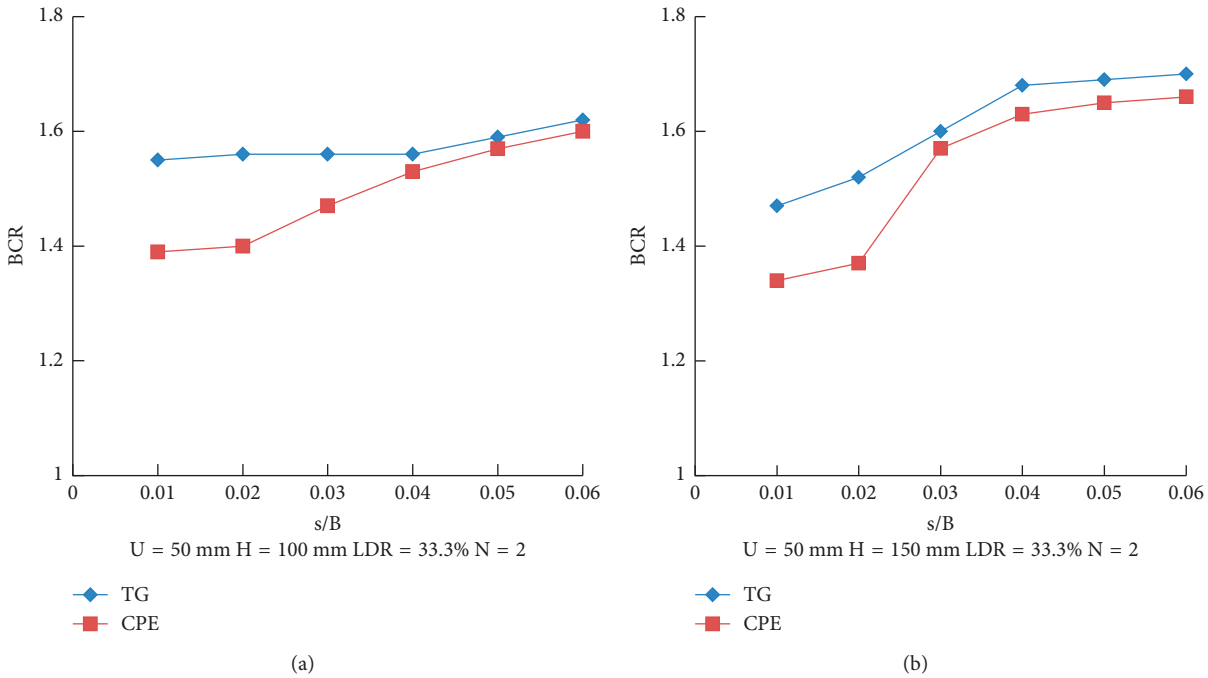

Figure 12: The relationship between BCR and geobelt type: (a) $U = 50$ mm, $H = 100$ mm, LDR = 33.3%, and $N = 2$; (b) $U = 50$ mm, $H = 150$ mm, LDR = 33.3%, and $N = 2$.

of the cushion and the corresponding SDR values at the proportional limit state and stable state. As can be seen in the table, the stress diffusion angle of reinforced cushions was obviously larger than that of unreinforced cushions. At the proportional limit state, SDR values spanned from 1.46 to 1.60, which means the stress diffusion angle was improved by 1.46– 1.60 times with geobelt reinforcement. At the limit state, SDR values spanned from 1.76 to 2.63, which means the stress diffusion angle was improved by 1.76–2.63 times. Current results are consistent with the result of Gabr et al. [29, 30] that the stress diffusion angle at the stable state was smaller than that at the proportional limit state.

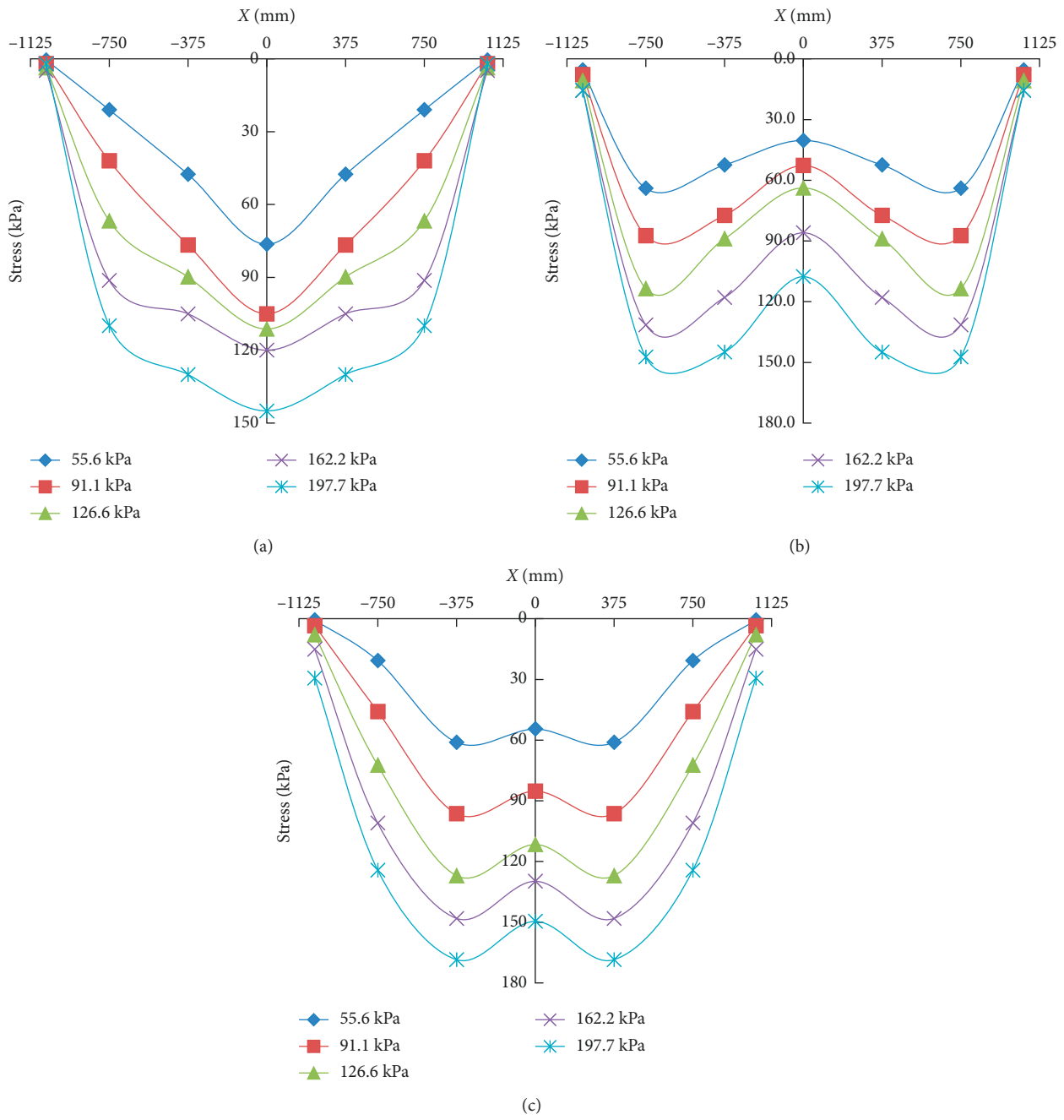

Figure 13: Stress distribution curves under the gravel cushion: (a) A0; (b) A1-1; (c) A2-2.

Figures 16–19 show the relationships between different parameters and the stress diffusion angle ratio. As can be seen in Figures 16(a) and 16(b), under same reinforcement conditions, the two-layer geobelt-reinforced cushion showed larger stress diffusion angle compared to the one-layer geobelt reinforced one. At the proportional limit state, SDR of the two-layer reinforced cushion was similar to that of the one-layer reinforced cushion, while at the stable state, there was a big difference between them. The reason is that, for two-layer geobelt reinforcement, first geobelt closer to the footing takes effect when the loading is small. As the loading increases, the second geobelt would then take its effect. Therefore, at the later stage of loading, the reinforcing effect of two-layer reinforcement became more pronounced. As can be seen in Table 6, at the stable state, SDRs spanned from 1.76 to 1.84 for the one-layer geobelt reinforced cushion, while for the two-layer geobelt reinforced cushion, the ratios were ranging from 2.46 to 2.63.

Figure 17 shows the relationship between the depth of the first geobelt layer beneath the footing (U) and SDR. Figure 18 shows the relationship between the linear density of reinforcement (LDR) and SDR. As can be seen, U and LDR had little impact on stress diffusion of the cushion. The possible reason is that the depth of the cushion adopted in

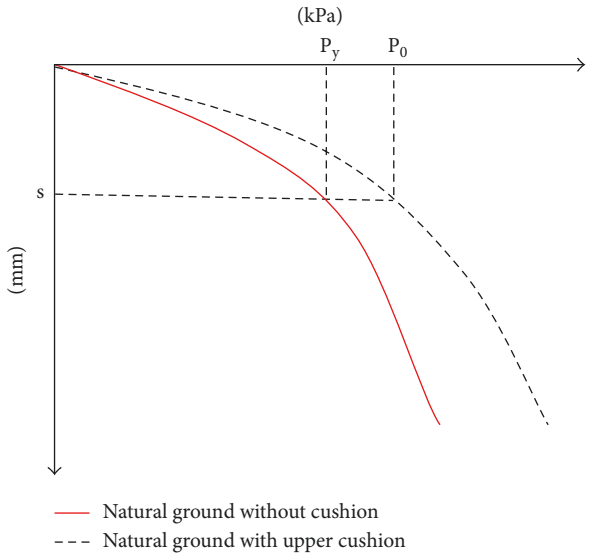

Figure 14: Calculation sketch of average earth pressure under the cushion.

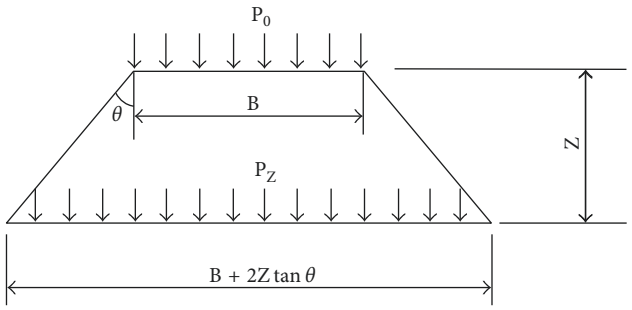

Figure 15: Stress diffusion of the cushion.

Table 6: The summary of stress diffusion angles.

Test number	Proportional limit state		Stable state	
	Angle (°)	SDR	Angle (°)	SDR
A0	38.8	1	18.9	1
A1-1	58.2	1.5	33.3	1.76
A1-2	57.4	1.48	34.8	1.84
A1-3	57.0	1.47	33.6	1.78
A1-4	57.0	1.47	33.5	1.77
A1-5	56.6	1.46	34.8	1.84
A2-1	62.1	1.60	48.0	2.54
A2-2	60.9	1.57	49.7	2.63
B2-1	58.6	1.52	46.7	2.46
B2-2	58.2	1.51	49.0	2.60

this study was small. As can be seen in Table 6, at the proportional limit state, the SDR decreased from 1.50 to 1.46 as U increased from 50 mm to 200 mm, while at the stable state, the SDR increased from 1.76 to 1.84 as U increased from 50 mm to 200 mm. It should be noted that the relationship between SDR and U is consistent with that between BCR and U. This also indicates that the geobelt only takes its effect efficiently after certain amount of deformation of cushion happens. The SDR was found to increase from 1.47 to 1.48 at the proportional limit state and increase from 1.77 to 1.84 at the stable state as the LDR increased from 25% to 50%. Therefore, the LDR showed unnoticeable effect on the stress diffusion of the geobelt reinforced cushion.

Figures 19(a) and 19(b) show the effect of vertical spacing between two geobelt layers (H) on the stress diffusion angle. For different types of geobelt, the values of SDR showed a similar trend, which is the stress diffusion angle increased slightly with the increase of H. At the proportional limit state, the SDRs of the TG-reinforced cushion were 1.57 and 1.60, while for the CPE-reinforced cushion, the values were 1.51 and 1.52, which is slightly smaller than that of the TG-reinforced cushion. At the stable state, the SDRs of the TG-reinforced cushion were 2.54 and 2.63, while for the CPE-reinforced cushion, the values were 2.46 and 2.60, which was also slightly smaller than that of the TG-reinforced cushion. It can be concluded that the reinforcing effect of TG geobelt was slightly better than that of CPE geobelt. The results are also consistent with BCR results discussed in Section 3.1.

4. Engineering Applications

In this section, a practical project included in *Technical code for ground treatment of buildings* [31] was presented to demonstrate the effect of geobelt.

The site of the project is located on a saturated silt soil with a bearing capacity of 80 kPa. The footing has a length and width of 60.8 m and 14.9 m, respectively. The thickness of the footing is 2.73 m. An average pressure beneath the footing is 130 kPa. Two possible treatment solutions are (1) unreinforced gravel cushion with a density of 19.5 kN/m^3, and the thickness of the cushion is taken as 3.73 m by calculation and (2) two-layer TG geobelt-reinforced thin gravel cushion. The density of the cushion was 19.5 kN/m^3. The width (B) was 17 m and thickness (Z) was 1.5 m with a Z/B ratio of 0.088 (<0.2). The project adopted the second treatment solution by using the geobelt-reinforced cushion. The first layer geobelt beneath the cushion was 0.6 m, and the vertical spacing between two layers was 0.4 m. The linear density reinforcement is 17%. According to the test results, the stress diffusion angle takes 35° considering a certain safety factor. After a comparative analysis, the reinforced cushion used in the second solution reduced the cushion thickness by 60% compared to the unreinforced cushion. The deformation after engineering settlement was 3.9 mm which meets the requirements.

According to this project, the stress diffusion angle of the reinforced gravel cushion was larger than that of the unreinforced one, which satisfies the bearing capacity and deformation requirements. In addition, the thickness of the cushion and construction cost can be reduced by using geobelt reinforcement.

5. Conclusions

By conducting the in situ square footing loading test on the geobelt-reinforced thin gravel cushion, this study investigated the reinforcing effect of geobelt on bearing capacity of the foundation and stress diffusion of cushions. The following conclusions can be made:

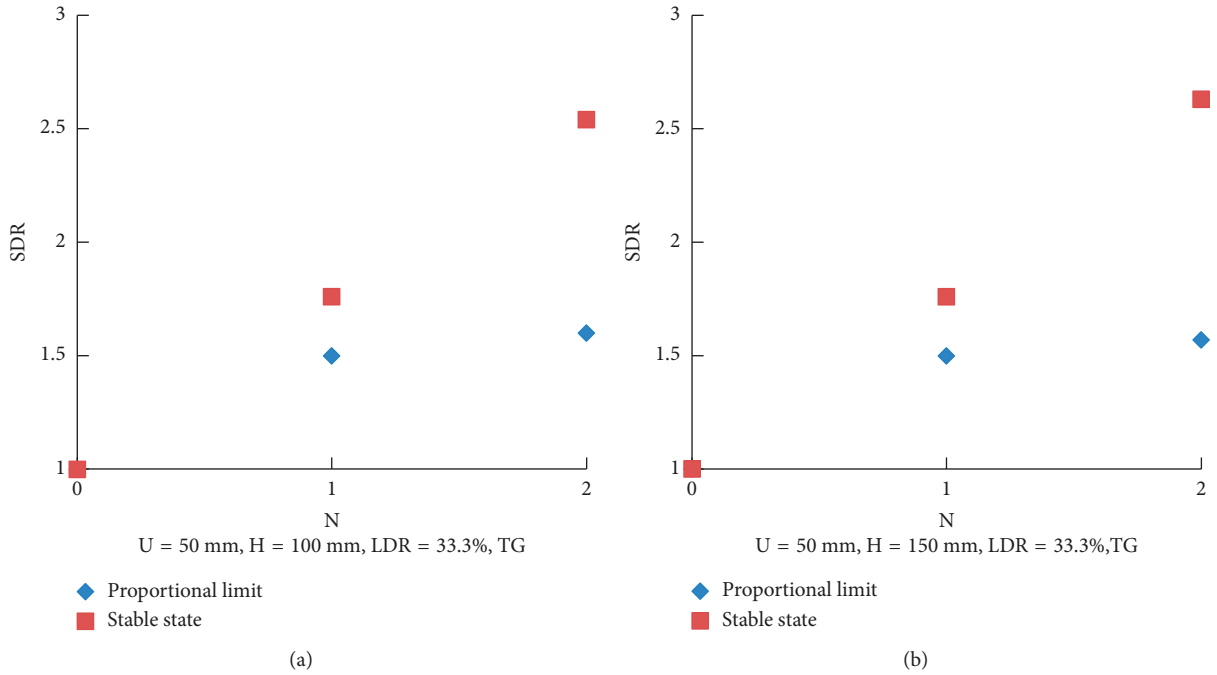

Figure 16: The relationships between SDR and N: (a) TG, $U = 50$ mm, $H = 100$ mm, and LDR = 33.3%; (b) TG, $U = 50$ mm, $H = 150$ mm, and LDR = 33.3%.

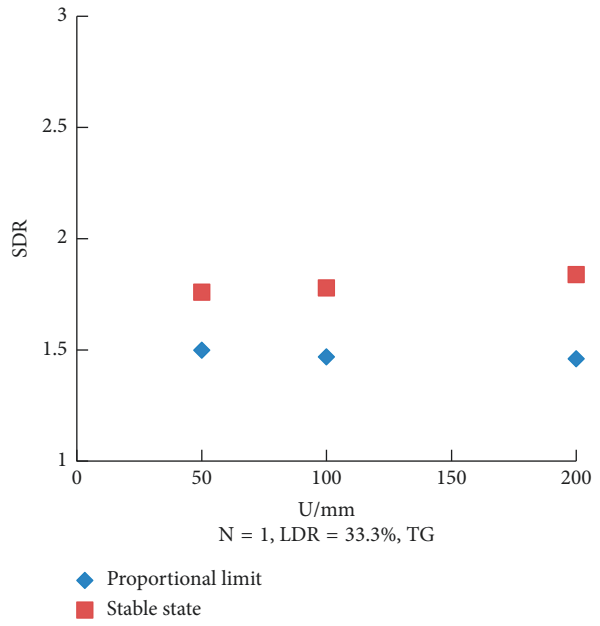

Figure 17: The relationship between SDR and U (TG; $N = 1$; LDR = 33.3%).

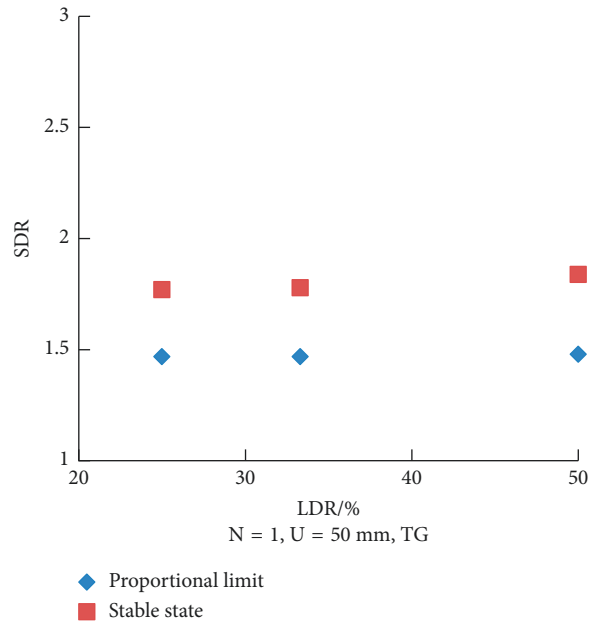

Figure 18: The relationship between SDR and LDR (TG; $N = 1$; $U = 50$ mm).

(1) Compared to unreinforced gravel cushions, geobelt reinforced cushions can improve the bearing capacity of foundation. The bearing capacity of one-layer geobelt-reinforced foundation was increased by 1.22–1.37 times while that of two-layer geobelt reinforced ones can be improved by 1.34–1.7 times.

(2) The earth pressure distribution on bottom of reinforced cushions was in a saddle shape, which was smoother than that of unreinforced cushions. When loaded, geobelt can restrict the movement of soils due to interfacial frictions between it and crushed gravels; therefore, the stress distribution of reinforced cushions becomes less varied compared to that of unreinforced cushions.

(3) The deformation and stress distribution of underlying soil layers under reinforced cushions were

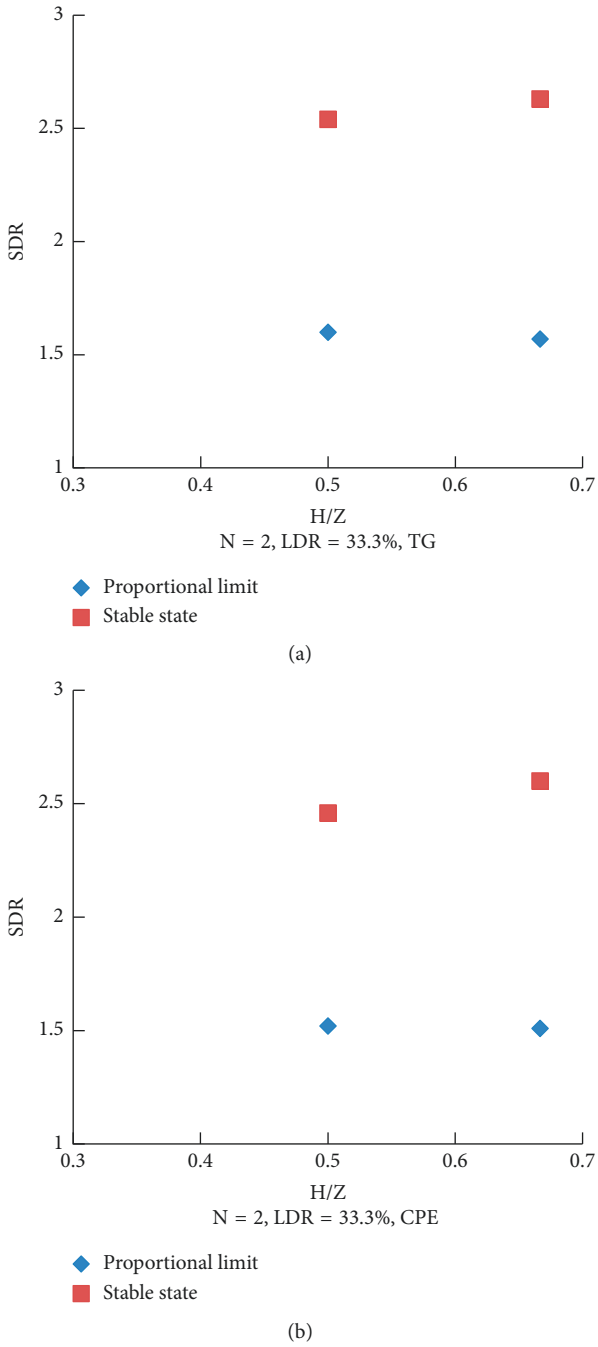

Figure 19: The relationship between SDR and H: (a) TG geobelt ($N = 2$; LDR = 33.3%); (b) CPE geobelt ($N = 2$; LDR = 33.3%).

much different from that under unreinforced cushions. Especially, the effect of geobelt on stress diffusion was pronounced. The stress diffusion angles of reinforced cushions were all larger than 20°.

(4) The reinforcing effect of two-layer geobelt reinforcement is obviously better than that of one-layer geobelt reinforcement. At the stable state, the stress diffusion angles of one-layer reinforced cushions were increased by 1.76–1.84 times while two-layer reinforcement was improved by 2.46–2.63 times, compared to unreinforced cushions.

(5) At the stable state, for the one-layer geobelt reinforced cushion, the stress diffusion and bearing capacity can be improved by increase of distance between the first geobelt and footing. A higher linear density of reinforcement can get a better bearing capacity and stress diffusion.

(6) At the stable state, for the two-layer geobelt reinforced cushion, the greater the vertical spacing between two layers, the better the stress diffusion effect and the larger the bearing capacity of the reinforced cushion. And the performance of the reinforced cushion with TG geobelt was better than that of the reinforced cushion with CPE geobelt.

Conflicts of Interest

The authors declare that they have no conflicts of interest.

References

[1] A. Kumar, M. L. Ohri, and R. K. Bansal, "Bearing capacity tests of strip footings on reinforced layered soil," *Geotechnical and Geological Engineering*, vol. 25, no. 2, pp. 139–150, 2007.

[2] A. Demir, A. Yildiz, and M. Laman, "Experimental and numerical analyses of circular footing on geogrid-reinforced granular fill underlain by soft clay," *Acta Geotechnica*, vol. 9, no. 4, pp. 711–723, 2014.

[3] B. M. Das, E. C. Shin, and M. T. Omar, "The bearing capacity of surface strip foundations on geogrid-reinforced sand and clay-a comparative study," *Geotechnical and Geological Engineering*, vol. 12, no. 1, pp. 1–14, 1994.

[4] G. M. Latha and A. Somwanshi, "Bearing capacity of square footings on geosynthetic reinforced sand," *Geotextiles and Geomembranes*, vol. 27, no. 4, pp. 281–294, 2009.

[5] S. N. M. Tafreshi, P. Sharifi, and A. R. Dawson, "Performance of circular footings on sand by use of multiple-geocell or -planar geotextile reinforcing layers," *Soils and Foundations*, vol. 56, no. 6, pp. 984–997, 2016.

[6] J. Binquet and K. L. Lee, "Bearing capacity tests on reinforced earth slabs," *Journal of Geotechnical Engineering Division*, vol. 101, pp. 1241–1256, 1975.

[7] J. Binquet and K. L. Lee, "Bearing capacity analysis on reinforced earth slabs," *Journal of Geotechnical Engineering Division*, vol. 101, pp. 1257–1276, 1975.

[8] C. C. Huang and F. Tatsuoka, "Bearing capacity of reinforced horizontal sandy ground," *Geotextiles and Geomembranes*, vol. 9, no. 1, pp. 51–80, 1990.

[9] C. C. Huang and F. Y. Meng, "Deep-footing and wide-slab effects in reinforced sandy ground," *Journal of Geotechnical and Geoenvironmental Engineering*, vol. 123, no. 1, pp. 30–36, 1997.

[10] A. Ghosh and A. K. Bera, "Bearing capacity of square footing on pond ash reinforced with jute-geotextile," *Geotextiles and Geomembranes*, vol. 23, no. 2, pp. 144–173, 2005.

[11] A. B. Cerato and A. J. Lutenegger, "Bearing capacity of square and circular footings on a finite layer of granular soil underlain by a rigid base," *Journal of Geotechnical and Geoenvironmental Engineering*, vol. 132, no. 11, pp. 1495–1501, 2006.

[12] G. M. Latha and A. Somwanshi, "Effect of reinforcement form on the bearing capacity of square footings on sand," *Geotextiles and Geomembranes*, vol. 27, no. 6, pp. 409–422, 2009.

[13] A. Demir, M. Laman, A. Yildiz, and M. Ornek, "Large scale field tests on geogrid-reinforced granular fill underlain by clay soil," *Geotextiles and Geomembranes*, vol. 38, no. 4, pp. 1–15, 2013.

[14] L. D. Suits, T. C. Sheahan, M. Abu-Farsakh, Q. Chen, R. Sharma, and X. Zhang, "Large-scale model footing tests on geogrid-reinforced foundation and marginal embankment soils," *Geotechnical Testing Journal*, vol. 31, no. 5, pp. 413–423, 2008.

[15] T. G. Sitharam, S. Sireesh, and S. K. Dash, "Model studies of a circular footing supported on geocell-reinforced clay," *Canadian Geotechnical Journal*, vol. 42, no. 2, pp. 693–703, 2011.

[16] M. Kiran and N. Bacha, "An experimental study on behaviour of bearing capacity and settlement of circular and square footing resting on reinforced sand bed stratified with lateritic soil," *International Journal of Engineering and Technical Research*, vol. 4, no. 6, 2015.

[17] R. Sharma, Q. Chen, M. Abu-Farsakh, and S. Yoon, "Analytical modeling of geogrid reinforced soil foundation," *Geotextiles and Geomembranes*, vol. 27, no. 1, pp. 63–72, 2009.

[18] M. G. Hussein and A. A. Meguid, "A three-dimensional finite element approach for modeling biaxial geogrid with application to geogrid-reinforced soils," *Geotextiles and Geomembranes*, vol. 44, no. 3, pp. 295–307, 2016.

[19] A. Kumar and S. Saran, "Closely spaced footings on geogrid-reinforced sand," *Journal of Geotechnical and Geoenvironmental Engineering*, vol. 129, no. 7, pp. 660–664, 2003.

[20] M. O. A. Bazne, F. Vahedifard, and S. Shahrokhabadi, "The effect of geonet reinforcement on bearing capacity of low-compacted soft clay," *Transportation Infrastructure Geotechnology*, vol. 2, no. 1, pp. 47–63, 2015.

[21] K. S. Sherin, S. Chandrakaran, and N. Sankar, "Effect of geocell geometry and multi-layer system on the performance of geocell reinforced sand under a square footing," *International Journal of Geosynthetic and Ground Engineering*, vol. 3, no. 3, p. 30, 2017.

[22] S. Biswas and S. Mittal, "Square footing on geocell reinforced cohesionless soils," *Geomechanics and Engineering*, vol. 13, no. 4, pp. 641–651, 2017.

[23] A. Kumar and A. Kaur, "A model tests of square footing resting on fibre-reinforced sand bed," *Geosynthetics International*, vol. 19, no. 5, pp. 385–392, 2012.

[24] D. Lal, N. Sankar, and S. Chandrakaran, "Effect of reinforcement form on the behaviour of coir geotextile-reinforced sand beds," *Soils and Foundation*, vol. 57, no. 2, pp. 227–236, 2017.

[25] B. M. Das and M. T. Omar, "The effects of foundation width on model tests for the bearing capacity of sand with geogrid reinforcement," *Geotechnical and Geological Engineering*, vol. 12, no. 2, pp. 131–141, 1994.

[26] Chinese Ministry of Housing and Urban-Rural Development, *Code for Design of Building Foundation*, Chinese Ministry of Housing and Urban-Rural Development, Beijing, China, 2011.

[27] M.T. Adams and J. G. Collin, "Large model spread footing load tests on geosynthetic reinforced soil foundations," *Journal of Geotechnical and Geoenvironmental Engineering*, vol. 123, no. 1, pp. 66–72, 1997.

[28] Q. Chen, M. Abu-Farsakh, and R. Sharma, "Experimental and analytical studies of reinforced crushed limestone," *Geotextiles and Geomembranes*, vol. 27, no. 5, pp. 357–367, 2009.

[29] M. A. Gabr, R. Dodson, and J. G. Collin, "A study of stress distribution in geogrid-reinforced sand," in *Proceeding of Geosynthetic in Foundation Reinforcement and Erosion Control Systems, ASCE*, pp. 62–76, Boston, MA, USA, October 1998.

[30] R. Chaney, K. Demars, M. Gabr, and J. Hart, "Elastic modulus of geogrid-reinforced sand using plate load tests," *Geotechnical Testing Journal*, vol. 23, no. 2, pp. 245–250, 2000.

[31] Chinese Ministry of Housing and Urban-Rural Development, *Technical Code for Ground Treatment of Buildings*, Chinese Ministry of Housing and Urban-Rural Development, Beijing, China, 2013.